Unconventional superconductivity and paramagnetic Meissner response triggered by nonlocal pairing interaction in proximitized heterostructures

A. A. Kopasov [1,2,*] and A. S. Mel'nikov [1,2,3]

[1] *Institute for Physics of Microstructures, Russian Academy of Sciences, 603950 Nizhny Novgorod, GSP-105, Russia*
[2] *Lobachevsky State University of Nizhny Novgorod, 603950 Nizhny Novgorod, Russia*
[3] *Moscow Institute of Physics and Technology, Dolgoprudnyi, Moscow Region 141701, Russia*

(Received 27 October 2023; revised 29 August 2024; accepted 30 August 2024; published 9 September 2024)

Proximity phenomena and induced superconducting correlations in heterostructures are shown to be strongly affected by the nonlocal nature of the electronic attraction. The latter can trigger the formation of Cooper pairs consisting of electrons localized in neighboring layers even in the absence of direct quasiparticle transfer between the layers. We investigate the manifestations of such nonlocal pairing and resulting unconventional induced superconductivity in an exemplary two-dimensional (2D) electronic system coupled to a conventional superconductor. The interplay between the quasiparticle tunneling and spin-triplet interlayer pairing is shown to generate the odd-frequency superconducting correlations in the 2D material which give rise to the paramagnetic contribution to the Meissner response and affect the energy resolved quasiparticle density of states. Experimental evidence for the above nonlocal interface pairing would provide new perspectives in engineering the unconventional superconducting correlations in heterostructures.

DOI: 10.1103/PhysRevB.110.094503

I. INTRODUCTION

For more than half a century the physics of proximity phenomena in various superconducting heterostructures remains an attractive research direction both for experimentalists and theoreticians. The key mechanism underlying the proximity effect is known to arise from the electron transfer between the superconducting and nonsuperconducting material which results in the generation of the induced superconducting correlations in the normal subsystem [1]. The structure of these correlations is determined not only by the order parameter of the primary superconductor but also by the properties of the quasiparticle excitations inside the nonsuperconducting material. As a result, manipulating the electronic spectrum of the latter we get a unique possibility to engineer the induced superconducting state. To tune, e.g., the spin structure of Cooper pairs one can exploit the effect of exchange field in ferromagnetic subsystems [2,3] or the spin-orbit effects arising at the interfaces in heterostructures or in noncentrosymmetric materials [4–8]. On this way we can get very exotic structure of superconducting correlations providing the possibility to control both the equilibrium and transport effects in superconducting heterostructures. These unconventional superconducting correlations are particularly interesting in the context of recent development of the field of topologically protected quantum computations [9,10] and superconducting spintronics [5–8].

Is the above mentioned electron transfer between the subsystems the only mechanism underlying the proximity effect in heterostructures? An obvious answer to this question is positive provided we disregard the nonlocal nature of the attraction between the electrons responsible for the superconductivity phenomenon. However, in real systems, this attractive interaction mediated, e.g., by phonons is not necessary local and can in principle bind the electrons even separated by the interface between the materials. In other words, the interface impenetrable for electrons can be still transparent for the phonons. Certainly, different crystal lattice structures of contacting solids and, thus, different elastic properties should result in the reflection of the elastic waves incident on the interface. This reflection as well as the screening effects are expected to weaken any attractive forces between the quasiparticles localized in neighboring subsystems. Still, if this nonlocal attraction is nonzero it can cause the formation of Cooper pairs of electrons positioned, e.g., in neighboring layers of the multilayered structure. This scenario of interlayer pairing is not completely new, of course, and previously it was discussed in the context of different layered superconductors such as transition metal dichalcogenides and high-T_c cuprates [11–16]. An important property of such interlayer pairing is that due to the nonlocality of the Cooper pair wave function (or more rigorously, the anomalous Green function) the Pauli principle does no more impose well known severe restrictions on the spins of electrons in the pair [17] which usually hamper the formation of triplet superconducting correlations. Exactly this argument in favour of possible triplet interlayer pairing motivated A. I. Larkin and K. B. Efetov [11] to consider this type of correlations to explain the extremely high upper critical fields in TaS_2 (pyridine) which were shown to exceed the paramagnetic limit [18]. These theoretical considerations of the interlayer pairing have been further developed [12–16] in the context of extensive studies of superconductivity in cuprates which also can be well described by the model of identical superconducting layers.

*Contact author: kopasov@ipmras.ru

All the above theoretical works were devoted to the study of natural layered compounds and, thus, assumed the coinciding electronic structure of the individual layers. Recent progress in the study of superconductivity in van der Waals heterostructures (see Refs. [19,20] and references therein) provides an interesting new possibility for engineering the superconducting state. Besides combining different materials in a hybrid structure, for identical layers in a stack the band structure is highly sensitive to a relative layer twist and can be also controlled by an external electric field. Such modifications of the electronic spectrum provides the way for electrostatic control of the superconducting state [21]. Existing theoretical studies of the superconducting order in van der Waals materials include the analysis of both intralayer and interlayer pairing correlations as well as the analysis of the spatial structure of the superconducting correlations in displaced bilayer graphene and transition metal dichalcogenides [22–25]. Rather common theoretical approach for considering the effects of the interlayer pairing is based on the assumption of the presence of an attractive interlayer interaction, which is treated similarly as in the BCS theory. Such an approach being rather general allows one to reveal qualitative effects of the interlayer superconductivity for a wide range of systems without reference to a specific mechanism of the interlayer pairing. Physical mechanisms underlying such nonlocal pairing are currently under theoretical investigation. In particular, for AA-stacked bilayer graphene, it has been shown that the interlayer Coulomb interaction can become attractive [26]. It has been also recently shown that magnons in the antiferromagnetic insulator sandwiched between two transition metal dichalcogenide monolayers can give rise to interlayer pairing with the resulting interlayer superconducting state of the form of coexisting *s*-wave and chiral *p*-wave [27].

The goal of our work is to apply the idea of Larkin and Efetov to the artificial heterostructures where the neighboring layers can possess quite different individual electronic characteristics including the difference in the normal state band spectra as well as different pairing properties. Considering the formation of the pairs consisting of electrons with different band spectra one can immediately notice the formal analogy of this problem to the one describing a standard singlet superconductor with the quasiparticle spectrum split by the Zeeman or exchange field. Certainly, the effective exchange field in our scenario will depend on the quasiparticle momentum but the basic features of the system including the depairing effect of the difference in the electronic spectra, formation of the odd-frequency superconducting correlations and the inhomogeneous Fulde-Ferrell-Larkin-Ovchinnikov (FFLO) state should be similar to the well known models describing the superconductors in the presence of the spin splitting field [3,28–32] (see also Ref. [33] and references therein). Let us emphasize that all these features are expected to appear in heterostructures without any ferromagnetic layers which could provide the source of the true exchange field determined by the interaction of electron spins with ferromagnetic ordering. This observation looks particularly interesting if we remind some rather old experiments indicating the presence of low temperature paramagnetic contribution to the Meissner response in superconducting cylinders covered by thin normal metal layers [34,35]. Several theoretical works argue that this phenomenon can be associated with the orbital effects [36], the electronic repulsion in the normal metal layer [37], the appearance of the *p*-wave superconductivity at low temperatures [38], and the effects of the spin-orbit interaction [39]. In view of the above discussion this paramagnetic response could originate also from the odd-frequency superconducting correlations generated by the nonlocal electron pairing according to the Larkin-Efetov mechanism. Another interesting application of the interlayer pairing arises if we consider its role in Majorana-type systems [40,41] where this mechanism can probably help to get rid of necessity of rather high magnetic fields providing the Zeeman splitting of energy band in Majorana nanowires. Motivated by all these arguments we studied the manifestation of the Larkin-Efetov mechanism in two exemplary systems: (i) a bilayer consisting of thin films with a certain energy shift of the conduction bands (ii) a two dimensional electron gas (2DEG) placed in contact with a thick superconducting layer (SC).

The paper is organized as follows. In Sec. II, we investigate the influence of tunneling and the band offset on the spin-singlet interlayer superconductivity and the electrodynamic response of the superconducting state within the framework of the two-layer model. In Sec. III, we reveal the manifestations of the interlayer spin-triplet superconductivity on the spectral and screening properties of the 2DEG in contact with a massive conventional superconductor. Finally, the results are summarized in Sec. IV.

II. TWO-LAYER MODEL

We proceed with the consideration of the phenomenon of interlayer pairing in a two layer model which can be viewed as the generalization of the one studied previously in Ref. [11]. The key point is that we assume the normal quasiparticle spectra to differ by a certain constant shift due to different conduction band offsets. For simplicity we neglect here the Cooper pairing in each individual layer. It is important to note that the considered two-layer model has some similarities with the model of a two-band superconductor with the interband pairing (see, e.g., Refs. [42,43]). In this regard, the interlayer pairing is a reminiscent of a cross-band pairing (or simply crosspairing) in multi-band models. However, the two models are not equivalent and the main difference is the presence of a tunable degree of the band hybridization in the two-layer model described by a finite hopping parameter. In a real experimental situation, the tunability of the layer coupling can be achieved by changing the thickness of the intermediate insulating layer. We expect that the intralayer pairing should compete with the interlayer one causing a non-BCS temperature dependencies of the order parameters as well as unusual temperature behavior of the kernels in the linear relationship between the supercurrent and the vector potential. Possible effects of intralayer pairing also include the temperature- and/or phase-offset driven phase transitions between the superconducting states with different relative phases of the order parameters [42,44]. These effects can also manifest themselves through pecularities in the behavior of the supercurrent response as function of temperature and the band offset.

A. Basic equations

The total Hamiltonian accounting for the interlayer pairing takes the form: $H = \sum_{j=1,2} H_j + H_t + H_{\text{int}}$, where

$$H_j = \int d^2\mathbf{r}\ \psi^\dagger_{j\sigma}(\mathbf{x})\hat{\xi}_j\psi_{j\sigma}(\mathbf{x}), \tag{1}$$

describe isolated two-dimensional layers, $\mathbf{x} = (\mathbf{r}, \tau)$, τ is the imaginary-time variable in the Matsubara technique, $\sigma =\uparrow,\downarrow$ denotes spin degrees of freedom (summation over repeated indices is implied), $\psi^\dagger_{j\sigma}(\mathbf{x})$ and $\psi_{j\sigma}(\mathbf{x})$ are fermionic creation and annihilation operators in the layer j in the Matsubara representation, respectively, $\hat{\xi}_j = -\nabla^2_{\mathbf{r}}/2m - \mu_j$, and m is the effective mass. The relative shift of the conduction bands is expressed as $(\mu_1 - \mu_2) = 2\chi$, where μ_j is the difference between the chemical potential and the bottom of the corresponding energy band. Our consideration is restricted to the case of momentum-conserving tunneling described by the term

$$H_t = \int d^2\mathbf{r}[t\psi^\dagger_{1\sigma}(\mathbf{r})\psi_{2\sigma}(\mathbf{x}) + t^*\psi^\dagger_{2\sigma}(\mathbf{r})\psi_{1\sigma}(\mathbf{x})]. \tag{2}$$

Note that the time-reversal symmetry imposes the following constraint on the hopping parameter $t = t^*$. The interlayer electron-electron interaction is described by the term

$$H_{\text{int}} = \frac{U_0}{2}\int d^2\mathbf{r}\ \psi^\dagger_{1\sigma}(\mathbf{x})\psi^\dagger_{2\sigma'}(\mathbf{x})\psi_{2\sigma'}(\mathbf{x})\psi_{1\sigma}(\mathbf{x}). \tag{3}$$

Assuming the existence of an attractive interlayer interaction with $U_0 = -|U_0|$ and treating the interlayer interaction within the mean-field approximation, one gets the effective interaction

$$H_{\text{eff}} = \int d^2\mathbf{r}\bigg[\frac{2}{|U_0|}\text{Tr}(\hat{\Delta}_{\text{int}}\hat{\Delta}^\dagger_{\text{int}}) + (\hat{\Delta}_{\text{int}})_{\sigma\sigma'}\psi^\dagger_{1\sigma}\psi^\dagger_{2\sigma'} + (\hat{\Delta}^*_{\text{int}})_{\sigma\sigma'}\psi_{2\sigma'}\psi_{1\sigma}\bigg], \tag{4}$$

in which $\hat{\Delta}_{\text{int}}$ is the 2×2 interlayer matrix gap function in the spin space.

Our analysis is based on the Gor'kov equation for the 8×8 matrix Green's function in the generalized layer-Nambu (particle-hole)-spin space

$$\underline{G}(\mathbf{x}_1, \mathbf{x}_2) = \langle T_\tau\underline{\psi}(\mathbf{x}_1)\underline{\psi}^\dagger(\mathbf{x}_2)\rangle. \tag{5}$$

Here T_τ is the time-ordering operator, $\underline{\psi} = [\psi_{1\uparrow}, \psi_{1\downarrow}, \psi^\dagger_{1\uparrow}, \psi^\dagger_{1\downarrow}, \psi_{2\uparrow}, \psi_{2\downarrow}, \psi^\dagger_{2\uparrow}, \psi^\dagger_{2\downarrow}]^{\text{T}}$, and the angular brackets stand for the thermodynamic average. The system's Green's function has the following structure in the layer space

$$\underline{G} = \begin{pmatrix} \check{G}_{11} & \check{G}_{12} \\ \check{G}_{21} & \check{G}_{22} \end{pmatrix}, \tag{6}$$

and the following one

$$\check{G}_{ij} = \begin{pmatrix} \hat{G}_{ij} & \hat{F}_{ij} \\ \hat{\bar{F}}_{ij} & \hat{\bar{G}}_{ij} \end{pmatrix}, \tag{7}$$

in the particle-hole space ($i, j = 1, 2$). For the derivation of the Gor'kov equations we use the equations of motion for the field operators in the Matsubara representation. Assuming the in-plane translational symmetry and spatially homogeneous interlayer pairing state, we obtain the following system of Gor'kov equations written in the Matsubara frequency-momentum representation

$$\begin{pmatrix} -i\omega_n + \check{\tau}_z\xi_{1\mathbf{k}} & \check{t} \\ \check{t}^\dagger & -i\omega_n + \check{\tau}_z\xi_{2\mathbf{k}} \end{pmatrix}\begin{pmatrix} \check{G}_{11} & \check{G}_{12} \\ \check{G}_{21} & \check{G}_{22} \end{pmatrix} = 1, \tag{8}$$

where $\omega_n = 2\pi T(n + 1/2)$, T is temperature, n is an integer, $\xi_{j\mathbf{k}} = \mathbf{k}^2/2m - \mu_j$, $\check{\tau}_i$ ($i = x, y, z$) are the Pauli matrices acting in the electron-hole space, and the coupling matrix $\check{t}$ is given by

$$\check{t} = \begin{pmatrix} t & \hat{\Delta}_{\text{int}} \\ -\hat{\Delta}^*_{\text{int}} & -t \end{pmatrix}. \tag{9}$$

One can see that the Green functions of the subsystems ($\check{G}_{11}$ and $\check{G}_{22}$) as well as the mixed ones ($\check{G}_{12}$ and $\check{G}_{21}$) acquire a nontrivial structure in the particle-hole space due to the presence of the interlayer gap function $\hat{\Delta}_{\text{int}}$, which satisfies the self-consistency equation

$$\hat{\Delta}_{\text{int}} = -\frac{U_0}{2}T\sum_{\omega_n}\int\frac{d^2\mathbf{k}}{(2\pi)^2}\hat{F}_{12}(\mathbf{k};\omega_n). \tag{10}$$

Equations (8), (9), and (10) form the basis for our analysis of the interlayer pairing in the two-layer model. In the following Sec. II B, we discuss the structure of the pairing correlations and analyze the behavior of the self-consistent interlayer pairing field as function of the relative band offset χ and temperature. In Sec. II C, we present the results regarding the influence of the interlayer pairing on the screening properties of the hybrid structure. For definiteness, the effects of the nonlocal Cooper pairing in the two-layer system are analyzed for an exemplary spin-singlet interlayer pairing

$$\hat{\Delta}_{\text{int}} = d_0(i\hat{\sigma}_y), \tag{11}$$

where $\hat{\sigma}_i$ ($i = x, y, z$) are the Pauli matrices acting in the spin-space.

B. Structure of the pairing correlations and the self-consistent solution for the interlayer order parameter

We proceed to the discussion of the structure of the pairing correlations in the two-layer system and our starting point is the Gor'kov Eq. (8)

$$(-i\omega_n + \check{\tau}_z\xi_{1\mathbf{k}})\check{G}_{11} + \check{t}\check{G}_{21} = 1, \tag{12a}$$

$$(-i\omega_n + \check{\tau}_z\xi_{1\mathbf{k}})\check{G}_{12} + \check{t}\check{G}_{22} = 0, \tag{12b}$$

$$(-i\omega_n + \check{\tau}_z\xi_{2\mathbf{k}})\check{G}_{22} + \check{t}^\dagger\check{G}_{12} = 1, \tag{12c}$$

$$(-i\omega_n + \check{\tau}_z\xi_{2\mathbf{k}})\check{G}_{21} + \check{t}^\dagger\check{G}_{11} = 0. \tag{12d}$$

Using Eqs. (9) and (11), we solve the above algebraic system and obtain both the intralayer and interlayer anomalous Green's functions $\hat{F}_{ij} = F_{ij}(i\hat{\sigma}_y)$

$$F_{11}(\mathbf{k}) = -2td_0\xi_{2\mathbf{k}}Z^{-1}(\mathbf{k}), \tag{13a}$$

$$F_{12}(\mathbf{k}) = d_0\big[-i\omega_n(\xi_{1\mathbf{k}} - \xi_{2\mathbf{k}}) + \omega_n^2 + \xi_{1\mathbf{k}}\xi_{2\mathbf{k}} + t^2 + d_0^2\big]Z^{-1}(\mathbf{k}). \tag{13b}$$

Here

$$Z(\mathbf{k}) = \left(\omega_n^2 + t^2 + d_0^2\right)^2 + \omega_n^2\left(\xi_{1\mathbf{k}}^2 + \xi_{2\mathbf{k}}^2\right) + \xi_{1\mathbf{k}}^2\xi_{2\mathbf{k}}^2 - 2\xi_{1\mathbf{k}}\xi_{2\mathbf{k}}\left(t^2 - d_0^2\right). \tag{14}$$

To obtain the functions F_{22} and F_{21}, one should interchange the layer indices $1 \leftrightarrow 2$ in Eqs. (13). Note that the denominator $Z(\mathbf{k})$ is symmetric with respect to this change. The poles of the resulting Green's functions together with the replacement $i\omega_n \to E$ give the quasiparticle spectrum of the two-layer system, which can be cast to the form

$$E_\pm^2(\mathbf{k}) = t^2 + |d_0|^2 + \xi_\mathbf{k}^2 + \chi^2 \pm 2\sqrt{\xi_\mathbf{k}^2(t^2 + \chi^2) + \chi^2|d_0|^2}, \tag{15}$$

with $\xi_\mathbf{k} = (\xi_{1\mathbf{k}} + \xi_{2\mathbf{k}})/2$.

The resulting Eqs. (13) and (14) demonstrate that in the general case the superconducting state of the hybrid system represents a mixture of the even- and odd-frequency spin-singlet superconducting correlations. The intralayer correlations [see Eq. (13a)] are even with respect to $\omega_n \to -\omega_n$ and are present only for a finite hopping parameter t. The interlayer superconducting correlations [see Eq. (13b)] have both even- and odd-frequency components. The even-frequency component is nonzero even in the absence of tunnel coupling between the layers, and the odd-frequency component of the interlayer correlations is proportional to $(\xi_{1\mathbf{k}} - \xi_{2\mathbf{k}})$ and appears only for a finite band offset χ.

Below we demonstrate the analogy between the effects of the band structure on nonlocal Cooper pairs and the ones of the spin-splitting field in a conventional superconductor by solving the self-consistency equation. Substituting the solution (13b) into Eq. (10) and using Eq. (15), we get

$$1 = -\frac{U_0}{4}T\sum_{\omega_n}\int\frac{d^2\mathbf{k}}{(2\pi)^2}\left[\frac{1}{\omega_n^2 + E_-^2} + \frac{1}{\omega_n^2 + E_+^2} \times \frac{-\chi^2}{\sqrt{\xi_\mathbf{k}^2|t|^2 + \chi^2\left(\xi_\mathbf{k}^2 + |d_0|^2\right)}}\left(\frac{1}{\omega_n^2 + E_-^2} - \frac{1}{\omega_n^2 + E_+^2}\right)\right]. \tag{16}$$

The form of the gap Eq. (16) is similar to the one for the superconductor with Rashba spin-orbit coupling under the influence of the Zeeman field (see, e.g., Eq. (27) in Ref. [45]). Thus we anticipate that a relative shift of the conduction bands should provide a depairing effect for interlayer Cooper pairs whereas the tunnel coupling mixes the states of isolated layers and should play a role similar to the spin-orbit interaction. For the solution of the self-consistency equation, we assume μ_j to be much larger than the cutoff energy Ω and then eliminate the cutoff in favor of the superconducting critical temperature of the interlayer order parameter $T_{c0}^{\rm int}$ at zero conduction band shift $\chi = 0$ [46]. The resulting gap equation reads

$$\ln\left(\frac{T}{T_{c0}^{\rm int}}\right) + 2\pi T\,\mathrm{Re}\sum_{\omega_n>0}\left[\frac{1}{\omega_n} - \frac{(|t|^2 + i\zeta)}{\zeta\sqrt{-\omega_n^2 - |d_0|^2 + \chi^2 + |t|^2 + 2i\zeta}}\right] = 0, \tag{17}$$

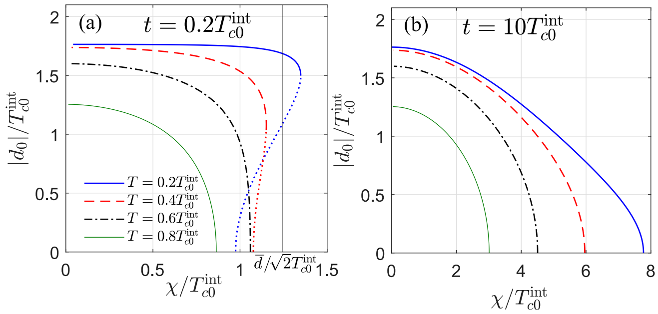

FIG. 1. The absolute value of the spin-singlet interlayer gap function $|d_0|$ for the two-layer model (8) vs the band splitting χ for $T/T_{c0}^{\rm int} = 0.2, 0.4, 0.6$, and 0.8. (a) and (b) correspond to $t/T_{c0}^{\rm int} = 0.2$ and 10, respectively. Unstable branches of the gap solution are shown by dotted lines. Here $T_{c0}^{\rm int}$ is the critical temperature for the interlayer order parameter at $\chi = 0$, t is the tunneling amplitude, and $\bar{d} = |d_0(T = 0)|$.

where $\zeta = \sqrt{\omega_n^2(|t|^2 + \chi^2) + |t|^2|d_0|^2}$. Typical $|d_0(\chi)|$ plots for different T shown in Fig. 1 demonstrate the suppression of the interlayer gap function by the band splitting. Figure 1(a) shows that for rather low temperatures and weak tunnel couplings there appear χ-regions with more than one solution of the gap equation, which is typical for the paramagnetic effect in superconductors. Thus, by the analogy with the spin-split superconductors [30–32], we argue that the relative band shift can lead to the appearance of the odd-frequency interlayer superconducting correlations and the FFLO instability. Note that this analogy is exact within the limit $t \to 0$. Figure 1(b) shows that the quasiparticle tunneling suppresses the depairing effect of the band splitting. Note also that if we now consider the joint effect of the relative band shift and the true Zeeman field, one can naturally expect the emergence of the reentrant superconductivity similar to the situation considered in Ref. [47].

Rigorous analysis of the superconducting state in the presence of multiple solutions to the gap equation requires calculations of the free energy and determination of stable and metastable states. However, the exact correspondence between the well-known model of spin-split superconductors [48] and the two-layer model for $t = 0$ provides a complete description of the influence of the band offset on the interlayer superconductivity in the absence of tunneling. In particular, for a homogeneous superconducting state at zero temperature, besides the trivial solution the gap equation has one solution for $|\chi| < \bar{d}/2$ and two solutions for $\bar{d}/2 < |\chi| < \bar{d}$. Here $\bar{d} = |d_0(T = 0)|$ denotes the absolute value of the interlayer gap function d_0 at zero temperature. The lower branch $d_0 = [\bar{d}(2\chi - \bar{d})]^{1/2}$ is characterized by a positive energy difference δE between the superconducting and the normal state. For the upper branch $d_0 = \bar{d}$ one has $\delta E \propto (2\chi^2 - \bar{d}^2)$ and the equilibrium superconductivity is realized only for $|\chi| < \bar{d}/\sqrt{2}$ [see Fig. 1(a)]. So, increasing the band offset χ from zero, the first-order transition into the normal state occurs at $\chi = \bar{d}/\sqrt{2}$. The χ region with multiple solutions of the gap equation shrinks upon the increase in temperature and starting from some finite temperature the transition from the normal to the superconducting state becomes of the second order for all relevant temperatures and band offsets. Our results (see Fig. 1) demonstrate that the situation is qualitatively similar to the above-described one only for rather small t and the first-order transition as a function of χ should be possible only for rather small T and t because the increase in the tunnel coupling also narrows the χ range with multiple solutions of the gap equation.

An alternative approach to establish the stability of the superconducting state in the presence of multiple solutions to the gap equation is to analyze the screening properties of the system for a particular solution. Indeed, the unstable solutions should reveal themselves via a total paramagnetic response of the supercurrent to the external magnetic field, which is unphysical in bulk superconducting systems (see Refs. [33,49–51] and references therein). Corresponding results of the linear response for the two-layer systems are presented in the next subsection. Let us note here that in our numerical calculations we observe that a nontrivial solution of the gap equation characterized by $\partial d_0/\partial\chi > 0$ [see, e.g., the results shown by dotted lines in Fig. 1(a)] provides a total paramagnetic response and is, thus, unstable.

Note also that the possibility of the band-offset induced FFLO instability in the two-layer system does not follow directly from our results shown in Fig. 1. Nevertheless, this statement is correct due to the exact correspondence between the two-layer model in the absence of tunneling and the model of spin-split superconductors. Study of the FFLO instability for finite tunnel couplings requires more sophisticated calculations and is behind the scope of our work.

C. Screening properties of the bilayer system

In this section, we provide the results regarding the linear response of the in-plane supercurrent in the two-layer system to the vector potential $\mathbf{A}(\mathbf{r})$ induced by an external magnetic field. The total current density represents the sum of current densities in the two layers and is given by the standard expression [52]

$$\mathbf{j}(\mathbf{r}) = \frac{ie}{m}\left[(\nabla_{\mathbf{r}} - \nabla_{\mathbf{r}'})T\sum_{n,j} G^{(1)}_{jj}(\mathbf{r},\mathbf{r}';\omega_n)\right]\Bigg|_{\mathbf{r}'\to\mathbf{r}} + \frac{2e^2}{m}\mathbf{A}(\mathbf{r})T\lim_{\tau\to -0}\sum_n G^{(0)}_{jj}(\mathbf{r},\mathbf{r};\omega_n)e^{-i\omega_n\tau}. \quad (18)$$

Here the upper subscripts denote the order of the perturbation correction for the Green's function with respect to the vector potential. Note that in the above expression we utilized a trivial structure of the normal intralayer Green's functions in the spin space. The first-order correction to the system's Green's function has the form

$$\underline{G}^{(1)}(\mathbf{r}_1,\mathbf{r}_2) = \frac{e}{2m}\int d\mathbf{r}'\,\underline{G}^{(0)}(\mathbf{r}_1,\mathbf{r}')\{\hat{\mathbf{p}}',\mathbf{A}(\mathbf{r}')\}\underline{G}^{(0)}(\mathbf{r}',\mathbf{r}_2), \quad (19)$$

in which the zero-order functions

$$\underline{G}^{(0)}(\mathbf{r}_1,\mathbf{r}_2) = \int\frac{d^2\mathbf{k}}{(2\pi)^2}\,\underline{G}^{(0)}(\mathbf{k})e^{i\mathbf{k}(\mathbf{r}_1-\mathbf{r}_2)}, \quad (20)$$

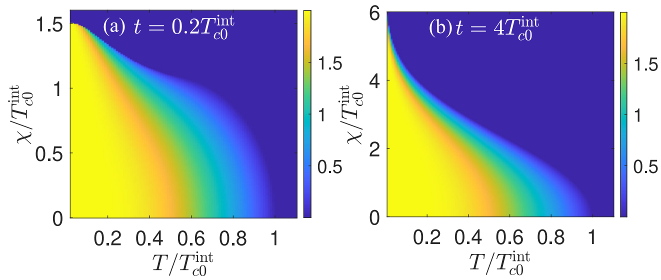

FIG. 2. Color plots of the coefficient $Q_{xx}(\mathbf{q}=0)$ defined by Eqs. (22) as functions of temperature and the band offset. The results are given in units $e^2v_F^2\nu_n$, where v_F denotes the Fermi velocity at $\chi=0$, and ν_n is density of states at the Fermi level. (a) and (b) refer to $t = 0.2T^{\rm int}_{c0}$ and $t = 4T^{\rm int}_{c0}$, respectively.

are defined by the solutions of the system (8). For the calculations of the current response we choose the transverse gauge for the vector potential $\nabla\mathbf{A} = 0$ and use the standard trick of adding and subtracting the normal-state contribution to the right-hand side of Eq. (18). Such procedure leads to cancellation of the second term in the right-hand side of Eq. (18) due to the fact that the total average number of particles is not affected by the transition into the superconducting state. We put

$$\mathbf{j}(\mathbf{r}) = \int\frac{d^2\mathbf{q}}{(2\pi)^2}\mathbf{j}(\mathbf{q})e^{i\mathbf{q}\mathbf{r}},\quad \mathbf{A}(\mathbf{r}) = \int\frac{d^2\mathbf{q}}{(2\pi)^2}\mathbf{A}(\mathbf{q})e^{i\mathbf{q}\mathbf{r}} \quad (21)$$

and arrive at rather lengty relation between the Fourier components of the supercurrent density and the vector potential

$$j_\alpha(\mathbf{q}) = -Q_{\alpha\beta}(\mathbf{q})A_\beta(\mathbf{q}), \quad (22a)$$

$$\begin{aligned}Q_{\alpha\beta}(\mathbf{q}) = \frac{2e^2}{m^2c}T\sum_n\int\frac{d^2\mathbf{k}}{(2\pi)^2}\,k_\alpha k_\beta \\ \times\big[G_{11}(\mathbf{k}_+)G_{11}(\mathbf{k}_-) + F_{11}(\mathbf{k}_+)\bar{F}_{11}(\mathbf{k}_-) \\ + G_{12}(\mathbf{k}_+)G_{21}(\mathbf{k}_-) + F_{12}(\mathbf{k}_+)\bar{F}_{21}(\mathbf{k}_-) \\ + G_{22}(\mathbf{k}_+)G_{22}(\mathbf{k}_-) + F_{22}(\mathbf{k}_+)\bar{F}_{22}(\mathbf{k}_-) \\ + G_{21}(\mathbf{k}_+)G_{12}(\mathbf{k}_-) + F_{21}(\mathbf{k}_+)\bar{F}_{12}(\mathbf{k}_-) \\ - \mathcal{G}_{11}(\mathbf{k}_+)\mathcal{G}_{11}(\mathbf{k}_-) - \mathcal{G}_{12}(\mathbf{k}_+)\mathcal{G}^{(0)}_{21}(\mathbf{k}_-) \\ - \mathcal{G}_{22}(\mathbf{k}_+)\mathcal{G}_{22}(\mathbf{k}_-) - \mathcal{G}_{21}(\mathbf{k}_+)\mathcal{G}^{(0)}_{12}(\mathbf{k}_-)\big]. \quad (22b)\end{aligned}$$

Here $\mathbf{k}_\pm = \mathbf{k}\pm\mathbf{q}/2$, the anomalous Green's function have the following structure in the spin space $\hat{F}_{ij} = F_{ij}(i\hat{\sigma}_y)$, $\hat{\bar{F}}_{ij} = \bar{F}_{ij}(-i\hat{\sigma}_y)$, and $\mathcal{G}_{ij}$ denote the Green's functions for $d_0 = 0$. Numerical calculation procedure includes the determination of the self-consistent solution for the gap equation followed by the momentum integration and the summation over the Matsubara frequencies in Eq. (22b).

Typical color plots of the coefficient in the linear relation between the supercurrent and the vector potential (22) as functions of temperature and the band offset are shown in Fig. 2. The results reveal the diagonal elements Q_{xx} (or Q_{yy}) evaluated at $\mathbf{q}=0$, and panels (a) and (b) correspond to $t = 0.2T^{\rm int}_{c0}$ and $t = 4T^{\rm int}_{c0}$, respectively. One can see that despite the presence of the odd-frequency superconducting correlations the total electromagnetic response of the two-layer system is diamagnetic throughout the entire superconducting region of the phase diagram. Our result is in qualitative agreement with the results of the generic model of multiorbital superconductors [53]. As it is shown previously, for a finite band offset the bilayer system possesses both even-and odd-frequency interlayer as well as the even-frequency intralayer superconducting correlations. The fact that both the normal and anomalous Green's functions in the right-hand side of Eq. (22b) depend on the interlayer pairing amplitude d_0 makes it complicated to separate the contributions from all relevant types of correlations into the screening properties of the two-layer system.

III. 2DEG IN CONTACT WITH A THICK *s*-WAVE SUPERCONDUCTOR

As a next step, we investigate the joint effect of the nonlocal pairing and the proximity induced superconductivity on the spectral properties and the Meissner response of 2DEG placed in contact with a thick SC layer. Our goal here is to demonstrate that one can obtain a nontrivial behavior of the density of states in 2DEG along with the paramagnetic contribution to the Meissner response. Although the structure of basic equations for 2DEG/SC model possess some similarities with previously considered two-layer model, for completeness below we provide an extensive description of the model equations.

A. Basic equations

Consider a two-dimensional electron gas ($z = 0$) proximity coupled to a conventional superconductor ($z > 0$). The Hamiltonian of the system reads

$$H = H_s + H_n + H_t + H_{\text{int}}, \tag{23}$$

with the first term

$$H_s = \int d^3\mathbf{R}[\psi^\dagger_{s\sigma}(\mathbf{X})\xi_s(\mathbf{R})\psi_{s\sigma}(\mathbf{X}) + \Delta_s(\mathbf{R})\psi^\dagger_{s\uparrow}(\mathbf{X})\psi^\dagger_{s\downarrow}(\mathbf{X}) + \Delta^*_s(\mathbf{R})\psi_{s\downarrow}(\mathbf{X})\psi_{s\uparrow}(\mathbf{X})], \tag{24}$$

describing the *s*-wave superconductor (SC) and the second term

$$H_n = d\int d^2\mathbf{r}\ \psi^\dagger_{n\sigma}(\mathbf{x})\xi_n(\mathbf{r})\psi_{n\sigma}(\mathbf{x}), \tag{25}$$

is the Hamiltonian of 2DEG. Here $\mathbf{X} = (\mathbf{R}, \tau)$, $\mathbf{x} = (\mathbf{r}, \tau)$, $\psi^\dagger_{s\sigma}(\mathbf{X})$ and $\psi_{s\sigma}(\mathbf{X})$ ($\psi^\dagger_{n\sigma}(\mathbf{x})$ and $\psi_{n\sigma}(\mathbf{x})$) are fermionic creation and annihilation operators in SC layer (2DEG) in the Matsubara representation, d is the thickness of the normal-metallic layer, $\xi_s(\mathbf{R}) = -\nabla^2_{\mathbf{R}}/2m_s - \mu_s$ and $\xi_n(\mathbf{r}) = -\nabla^2_{\mathbf{r}}/2m_n - \mu_n$ stand for the quasiparticle kinetic energy operators in the SC and 2DEG with respect to the corresponding chemical potentials μ_s and μ_n, m_s and m_n are the effective masses of the electrons in the subsystems, and $\Delta_s(\mathbf{r})$ is the superconducting gap function in the SC layer. The creation and annihilation operators in 2DEG are normalized to the layer volume $[\psi_{n\sigma}(\mathbf{r}, \tau), \psi^\dagger_{n\sigma'}(\mathbf{r}', \tau)] = d^{-1}\delta_{\sigma\sigma'}\delta(\mathbf{r} - \mathbf{r}')$.

The tunnel Hamiltonian has the form:

$$H_t = dt\int d^2\mathbf{r}[\psi^\dagger_{s\sigma}(\mathbf{x})\psi_{n\sigma}(\mathbf{x}) + \psi^\dagger_{n\sigma}(\mathbf{x})\psi_{s\sigma}(\mathbf{x})], \tag{26}$$

where $t \in \mathbb{R}$ is the tinneling matrix element and we denote $\psi_{s\sigma}(\mathbf{x}) = \psi_{s\sigma}(\mathbf{r}, z = 0, \tau)$ for brevity. Assuming that the interlayer attractive interaction is relevant in the vicinity of the SC/2DEG interface, we choose the following form of the interaction:

$$H_{\text{int}} = \frac{U_0}{2}d\int d^2\mathbf{r}\ \psi^\dagger_{s\sigma}(\mathbf{x})\psi^\dagger_{n\sigma'}(\mathbf{x})\psi_{n\sigma'}(\mathbf{x})\psi_{s\sigma}(\mathbf{x}). \tag{27}$$

Neglecting the back action of 2DEG on the superconductor and the effects of the interlayer interaction in SC layer, we derive the following Gor'kov equations for the Matsubara Green's functions in 2DEG written in the cooordinate-Matsubara frequency representation (see Appendix for details of the derivation):

$$[-i\omega_n + \check{\tau}_z\xi_n(\mathbf{r}_1)]\check{G}_n(\mathbf{r}_1, \mathbf{r}_2) - \int d^2\mathbf{r}\ \check{\Sigma}(\mathbf{r}_1, \mathbf{r})\check{G}_n(\mathbf{r}, \mathbf{r}_2) = d^{-1}\delta(\mathbf{r}_1 - \mathbf{r}_2), \tag{28a}$$

$$\check{\Sigma}(\mathbf{r}_1, \mathbf{r}) = d\check{t}\check{G}_s(\mathbf{r}_1, \mathbf{r})\check{t}^\dagger, \tag{28b}$$

Here $\check{G}_s(\mathbf{r}_1, \mathbf{r})$ stands for the Green's function of an isolated SC layer taken at the SC/2DEG interface $z_1 = z = 0$. The 4×4 matrix Green's function in Eq. (28a) has the following structure in the particle-hole space:

$$\check{G} = \begin{pmatrix} \hat{G} & \hat{F} \\ \hat{\bar{F}} & \hat{\bar{G}} \end{pmatrix}. \tag{29}$$

The presence of the interlayer pairing results in a nontrivial structure of the coupling matrix

$$\check{t} = \begin{pmatrix} t & \hat{\Delta}_{\text{int}} \\ -\hat{\Delta}^*_{\text{int}} & -t \end{pmatrix}, \tag{30}$$

which is similar to the previously studied two-layer mode. The interlayer gap function $\hat{\Delta}_{\text{int}}$ is defined through the relation

$$[\hat{\Delta}_{\text{int}}(\mathbf{r})]_{\sigma\sigma'} = -\frac{U_0}{2}\langle\psi_{n\sigma}(\mathbf{x})\psi_{s\sigma'}(\mathbf{x})\rangle. \tag{31}$$

Note that Eqs. (28) can be significantly simplified when the characteristic interatomic distance in the SC layer a_0 is much less than the one in 2DEG [54]. Indeed, for rapidly oscillating Green's function in the SC layer

$$\check{G}_s(\mathbf{r}_1, \mathbf{r}) = \frac{m_s}{2\pi}\left\{\check{\tau}_z\frac{\cos(k_{Fs}|\mathbf{r}_1-\mathbf{r}|)}{|\mathbf{r}_1-\mathbf{r}|} + \check{g}_s(\omega_n)\frac{\sin(k_{Fs}|\mathbf{r}_1-\mathbf{r}|)}{|\mathbf{r}_1-\mathbf{r}|}\right\} \times e^{-\frac{m_s\sqrt{\omega_n^2+|\Delta_s|^2}}{k_{Fs}}|\mathbf{r}_1-\mathbf{r}|}, \tag{32}$$

the integral in Eq. (28a) converges at $|\mathbf{r}_1 - \mathbf{r}| \sim a_0$, and the resulting self-energy is local. Thus, under our model assumptions, Eqs. (28) can be cast to the form

$$[-i\omega_n + \check{\tau}_z\xi_n(\mathbf{r}_1) - \check{\Sigma}(\omega_n)]\check{G}_n(\mathbf{r}_1, \mathbf{r}_2) = d^{-1}\delta(\mathbf{r}_1 - \mathbf{r}_2), \tag{33a}$$

$$\check{\Sigma}(\omega_n) = \pi d\nu_s a_0^2\check{t}^\dagger\check{g}_s(\omega_n)\check{t}, \tag{33b}$$

where k_{Fs} is the Fermi momentum in the normal-metal state of the SC layer, $\nu_s = m_s k_{F_s}/2\pi^2$ is the density of states per spin projection in the normal-metal state of the superconductor,

$$\check{g}_s(\omega_n) = \frac{i\omega_n - |\Delta_s|\hat{\sigma}_y\check{\tau}_y}{\sqrt{\omega_n^2 + |\Delta_s|^2}}, \tag{34}$$

is the quasiclassical Green's function in the SC layer.

The resulting Eqs. (33) are the basic equations for our analysis of the influence of the interlayer pairing in 2DEG/SC hybrid systems. In particular, we investigate the manifestations of the spin-triplet interlayer pairing and take as a model example

$$\hat{\Delta}_{\rm int} = d_t\hat{\sigma}_z(i\hat{\sigma}_y) = d_t\hat{\sigma}_x, \tag{35}$$

where d_t is the interlayer pairing amplitude. For simplicity, we choose the interlayer interaction amplitude d_t to be a real number. In calculations it is convenient to absorb the dimensional factors in the self-energy part (33b) into the definitions of t and d_t

$$\pi d\nu_s t^2 a_0^2 \to t^2, \tag{36a}$$

$$\pi d\nu_s d_t^2 a_0^2 \to d_t^2, \tag{36b}$$

$$\pi d\nu_s t d_t a_0^2 \to t d_t, \tag{36c}$$

so that the parameters t^2, d_t^2, and td_t in further consideration are given in the energy units.

B. Structure of the superconducting correlations and the density of state in 2DEG

In this section, we consider the effects of the spin-triplet interlayer pairing (35) on the spectral properties of the two-dimensional layer. First, we discuss the structure of the resulting self-energy (33b) and then analyze the energy dependence of the density of states in 2DEG. The results provided in this section refer to the case of zero external magnetic field.

Substitution of Eqs. (34) and (35) into Eq. (33b) yields the following form of the self-energy matrix in the particle-hole space

$$\check{\Sigma} = \begin{pmatrix} \hat{\Sigma}_{11} & \hat{\Sigma}_{12} \\ \hat{\Sigma}_{21} & \hat{\Sigma}_{22} \end{pmatrix}, \tag{37}$$

with

$$\hat{\Sigma}_{11}(\omega_n) = \frac{i\omega_n\left(t^2 + d_t^2\right)}{\sqrt{\omega_n^2 + |\Delta_s|^2}} + \frac{2td_t\Delta_s\hat{\sigma}_z}{\sqrt{\omega_n^2 + |\Delta_s|^2}}, \tag{38a}$$

$$\hat{\Sigma}_{12}(\omega_n) = \frac{-\Delta_s\left(t^2 + d_t^2\right)(i\hat{\sigma}_y)}{\sqrt{\omega_n^2 + |\Delta_s|^2}} - \frac{2i\omega_n t d_t\hat{\sigma}_x}{\sqrt{\omega_n^2 + |\Delta_s|^2}}. \tag{38b}$$

Note that in the above expressions $\check{\Sigma}$ represents a diagonal component of the self-energy in the layer space related to the 2DEG and its structure in terms of the spin indices is defined by the Pauli matrices $\hat{\sigma}_i$ ($i = x, y, z$). The other components $\hat{\Sigma}_{22}$ and $\hat{\Sigma}_{21}$ can be obtained from Eqs. (38) via the relations

$$\hat{\Sigma}_{22}(\omega_n) = -\hat{\Sigma}_{11}^{\rm T}(-\omega_n), \tag{39a}$$

$$\hat{\Sigma}_{21}(\omega_n) = \hat{\Sigma}_{12}^{\dagger}(-\omega_n). \tag{39b}$$

The off-diagonal matrix elements in the Nambu space $\hat{\Sigma}_{12}$ and $\hat{\Sigma}_{21}$ carry the information about the spin structure and the frequency dependence of the superconducting correlations in 2DEG. The first term in the right-hand side of Eq. (38b) illustrates the fact that the spin-triplet interlayer interaction results in the enhancement of the amplitude of the spin-singlet superconducting correlations in 2DEG. It is remarkable that the spin-singlet correlations in 2DEG survive in the limit $t \to 0$, so the interlayer interaction itself represents a mechanism for transferring the spin-singlet superconducting correlations from the superconductor to the two-dimensional layer. Considering the second term in Eq. (38b), we see that in the presence of the electron tunneling and the interlayer spin-triplet pairing, the two-dimensional system features the additional spin-triplet odd-frequency superconducting correlations. Finally, one can see that diagonal matrix elements $\hat{\Sigma}_{11}$ and $\hat{\Sigma}_{22}$ given by Eqs. (38a) and (39a) contain the additional Zeeman-like terms $\propto td_t\Delta_s\hat{\sigma}_z$. Correspondingly, the spin-triplet superconducting correlations in 2DEG can be accompanied by an additional spin splitting for quasiparticles in the two-dimensional system provided that it is coupled to the superconducting layer.

The above described features of the quasiparticle energy spectrum in 2DEG in the presence of the spin-triplet interlayer pairing imply the appearance of the multi-peak structure in the energy dependence of the density of states

$$\nu_{\rm 2D}(E) = \frac{1}{\pi}{\rm Im}{\rm Tr}[\hat{G}_n(\mathbf{R}, \mathbf{R}; \omega_n \to -iE + \eta)]. \tag{40}$$

Here the trace is taken over the spin indices and η is an infinitesimally small positive number. For the calculations of the density of states, we solve Eq. (33) with a local self-energy given by Eqs. (37)–(39). As a first step, we derive the expression for the normal Matsubara Green's function in 2DEG at coincident spatial arguments

$$[\hat{G}_n(\mathbf{R}, \mathbf{R})]_{\sigma\sigma} = \int \frac{d^2\mathbf{p}}{(2\pi)^2} \frac{[i(\tilde{\omega}_n - i\sigma h) + \xi_n]}{\left[\xi_n^2 + (\tilde{\omega}_n - i\sigma h)^2 + f_\sigma^2\right]}, \tag{41}$$

where $\sigma = \uparrow, \downarrow$ (± 1), $\xi_n = \mathbf{p}^2/2m_n - \mu_n$, and

$$\tilde{\omega}_n(\omega_n) = \omega_n\left(1 + \frac{t^2 + d_t^2}{\sqrt{\omega_n^2 + \Delta_s^2}}\right), \tag{42a}$$

$$h(\omega_n) = \frac{2td_t\Delta_s}{\sqrt{\omega_n^2 + \Delta_s^2}}, \tag{42b}$$

$$f_\sigma(\omega_n) = \frac{\Delta_s\left(t^2 + d_t^2\right) + 2i\sigma\omega_n t d_t}{\sqrt{\omega_n^2 + \Delta_s^2}}. \tag{42c}$$

Integration over the momentum in Eq. (41) gives

$$[\hat{G}_n(\mathbf{R}, \mathbf{R})]_{\sigma\sigma} = \pi\nu_n \frac{i\tilde{\omega}_n + \sigma h}{\sqrt{f_\sigma^2 - (i\tilde{\omega}_n + \sigma h)^2}}. \tag{43}$$

Here $\nu_n = m_n/2\pi$ is the density of states in an isolated 2DEG per spin projection. Finally, we substitute Eqs. (43) into Eq. (40) and calculate the density of states.

Typical behavior of the density of states in 2DEG as a function of energy and model parameters are presented in Fig. 3. Panels (a)–(c) show the color plots of the density of states as a function of energy E and the interlayer gap function d_t for several tunneling rates $t^2 = 0$, $t^2 = \Delta_s$, and $t^2 = 3\Delta_s$, respectively. Panels (d)–(f) reveal $\nu_{\rm 2D}(E)$ plots for several values of the interlayer gap function. We choose the energy level broadening parameter $\eta = 0.01\Delta_s$ to produce the plots. Figures 3(a)

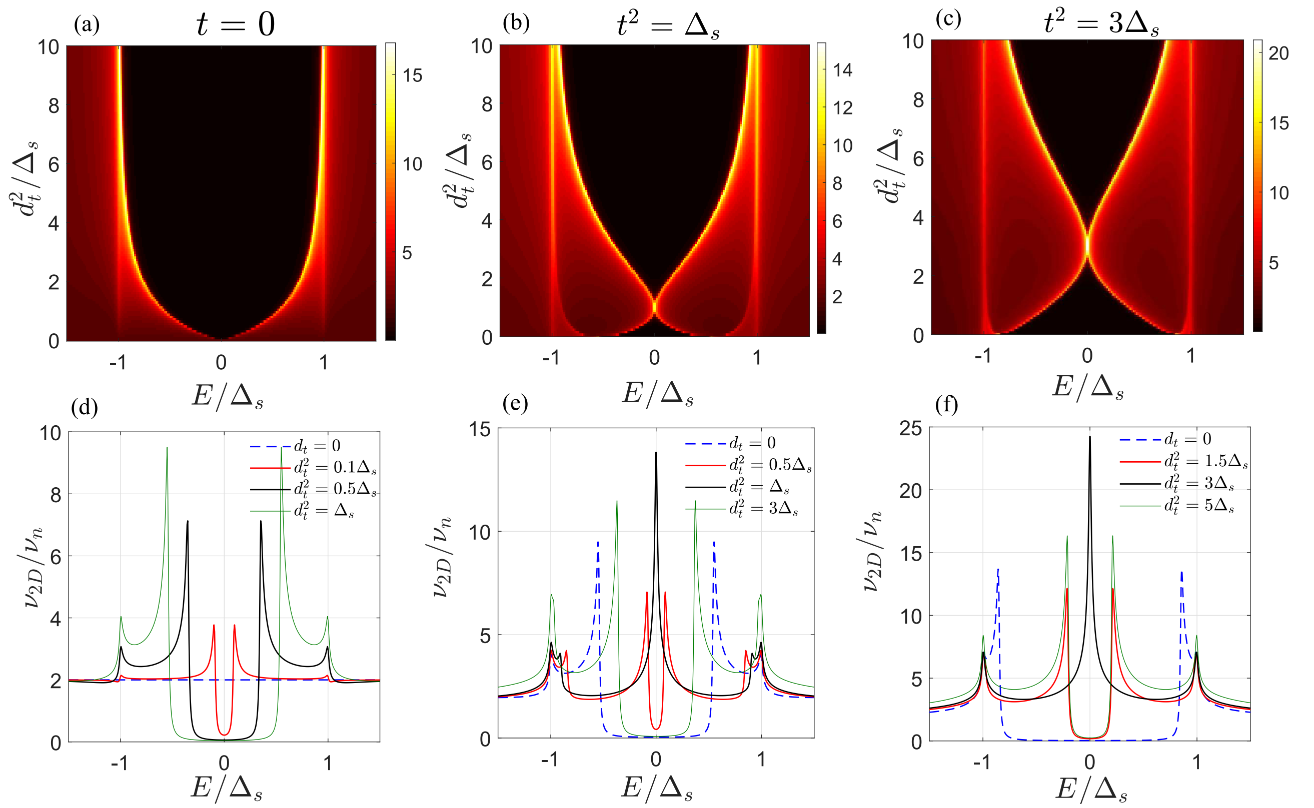

FIG. 3. Typical energy dependencies of the density of states in the two-dimensional layer ν_{2D}/ν_n, where ν_n is the density of states at the Fermi level per spin projection of an isolated 2DEG. [(a)–(c)] Color plots of the density of states as a function of energy E and the interlayer gap function d_t for several values of the tunneling rate t^2. [(d)–(f)] $\nu_{2D}(E)$ dependencies for various values of the interlayer gap function d_t. (a) and (d), (b) and (e), and (c) and (f) correspond to $t = 0$, $t^2 = \Delta_s$, and $t^2 = 3\Delta_s$, respectively. We choose the energy level broadening parameter $\eta = 0.01\Delta_s$ to produce the plots.

and 3(d) refer to the case $t = 0$, for which the two-dimensional layer only features the spin-singlet superconducting correlations [see Eq. (38b)]. One can see the emerging minigap in the density of states for rather small d_t values [see the solid red line in Fig. 3(d)]. The magnitude of the minigap for $d_t^2 = 0.1\Delta_s$ is approximately $0.2\Delta_s$, which is in agreement with the result of Eq. (38b) in the case $t = 0$ and $d_t^2 \ll \Delta_s$. Two additional features in the density of states are located near the energy gap of the parent superconductor $E \approx \pm\Delta_s$. The color plot in Fig. 3(a) shows that the spectral gap tends to $2\Delta_s$ upon the increase in the absolute value of the interlayer gap function. We provide $\nu_{2D}(E)$ plots for a finite tunneling rate $t^2 = \Delta_s$ and $d_t^2/\Delta_s = 0$, 0.5, 1, and 3 in Fig. 3(e). Corresponding $\nu_{2D}(E)$ curve for $d_t = 0$ (shown by a blue dashed line) represents a typical energy dependence of the density of states of 2DEG with the induced superconductivity and possesses two pair of peaks, one of which (at $E \approx \pm 0.55\Delta_s$) marks the induced hard gap in the energy spectrum and another one is located at $E \approx \pm\Delta_s$. The increase in the interlayer gap function leads to the splitting of the peaks at the parent gap and to the decrease in the induced gap, which eventually disappears at a certain value of interlayer pairing amplitude. The black solid line in Fig. 3(e) shows a pronounced zero-bias peak in the density of states at $d_t^2 \approx t^2$. The color plot in Fig. 3(b) demonstrates that the spectral gap reopens upon further increase in d_t and tends to $2\Delta_s$ for rather large d_t values. The results in Figs. 3(c) and 3(f) obtained for larger tunneling rate $t^2 = 3\Delta_s$ also demonstrate the hard gap closing-reopening feature upon the variation of the interlayer pairing amplitude as well as the appearance of a zero-bias peak in the density of states of the two-dimensional system at $d_t^2 = t^2$.

C. Screening properties of the induced superconducting correlations in 2DEG

We continue with the analysis of a linear response of the induced superconducting correlations in 2DEG to an external magnetic field. Corresponding linear relations between the supercurrent $\mathbf{j}$ and the vector potential $\mathbf{A}$ in 2DEG are derived within both the clean and dirty limit. For the derivation we choose the transverse gauge for the vector potential $\mathrm{div}\mathbf{A} = 0$ and follow the approach described in Ref. [55]. The validity of the obtained results is restricted to the case when the characteristic interatomic scale in 2DEG is much less than the spatial scale of the induced superconducting correlations. We stress that our results regarding the paramagnetic response of 2DEG coupled to massive superconductor is just the contribution of the 2DEG to the total response, which is, of course, diamagnetic due to a large diamagnetic response of a massive superconductor.

1. Clean limit

Here we consider the ballistic case. For the derivation of the quasiclassical equations in 2DEG, we introduce the

Matsubara Green's functions in the mixed representation

$$\check{G}_n(\mathbf{R},\mathbf{p}) = \int d\delta\mathbf{R}\, e^{-i\mathbf{p}\delta\mathbf{R}}\check{G}_n(\mathbf{R},\delta\mathbf{R}), \tag{44}$$

where $\mathbf{R} = (\mathbf{R}_1 + \mathbf{R}_2)/2$ and $\delta\mathbf{R} = \mathbf{R}_1 - \mathbf{R}_2$. Using Eqs. (28a), (44) and considering the quasiparticle states in the vicinity of the Fermi surface

$$\mathbf{p} = \mathbf{n}(p_{Fn} + \xi_n/v_{Fn}), \tag{45}$$

we derive the quasiclassical equations for the Green's function in the mixed representation

$$\left[-i\omega_n + \check{\tau}_z\left(\xi_n - \frac{i}{2}\mathbf{v}_{Fn}\nabla_{\mathbf{R}}\right) - e\mathbf{v}_{Fn}\mathbf{A}\left(\mathbf{R} + \frac{i}{2}\mathbf{v}_{Fn}\frac{d}{d\xi_n}\right)\right]\check{G}_n(\mathbf{R},\mathbf{n},\xi_n) - \check{\Sigma}(\mathbf{R})\check{G}_n(\mathbf{R},\mathbf{n},\xi_n) = 1. \tag{46}$$

Here $\mathbf{v}_{Fn} = v_{Fn}\mathbf{n}$, v_{Fn} denotes the Fermi velocity in an isolated 2DEG, $\mathbf{n} = [\cos\varphi_{\mathbf{p}}, \sin\varphi_{\mathbf{p}}, 0]$, $p_{Fn} = m_n v_{Fn}$, and ξ_n is the kinetic energy of quasiparticles relative to the chemical potential. Note that in the above equation we used the local approximation for the self-energy. The supercurrent density is then determined from the solution of Eq. (46)

$$\mathbf{j}(\mathbf{R}) = -ep_{Fn}T\sum_{\omega_n}\int\frac{d\xi_n}{(2\pi)}\frac{d\mathbf{n}}{(2\pi)}\mathbf{n}\mathrm{Tr}[\hat{G}_n(\mathbf{R},\mathbf{n},\xi_n)]. \tag{47}$$

As a next step, we find the first-order correction for the Green's function with respect to the vector potential. For this purpose, it is convenient to calculate the Fourier transform of the Green's function with respect to ξ_n

$$\check{G}_n(q) = \int \check{G}_n(\xi_n)e^{iq\xi_n}\frac{d\xi_n}{2\pi}. \tag{48}$$

Using Eq. (46), we derive the quasiclassical equation for the Fourier transform (48). Eliminating the spatial derivative via the replacement $\mathbf{R} \to \mathbf{R} - \frac{1}{2}\mathbf{v}_{Fn}q$, we get the equation

$$\left[-i\omega_n - i\check{\tau}_z\frac{\partial}{\partial q} - e\mathbf{v}_{Fn}\mathbf{A}(\mathbf{R} + q\mathbf{v}_{Fn})\right]\check{G}_n(q) - \check{\Sigma}\left(\mathbf{R} + \frac{1}{2}q\mathbf{v}_{Fn}\right)\check{G}_n(q) = \delta(q). \tag{49}$$

It is important to note that for the derivation of the linear response it is sufficient to expand the Green's function up to the first-order term in the vector potential

$$\check{G}_n(q) \approx \check{G}_n^{(0)}(q) + \check{G}_n^{(1)}(q), \tag{50}$$

and take the unperturbed homogeneous self-energy $\check{\Sigma}^{(0)}$ given by Eqs. (37)–(39). Indeed, within the local approximation the self-energy involves the Green's function in the superconducting layer at coincident spatial arguments. Therefore the first-order correction $\check{\Sigma}^{(1)}$ vanishes upon averaging over the momentum directions. Unperturbed Green's functions have the form

$$\hat{G}_n^{(0)}(q) = \sum_{\sigma=\uparrow,\downarrow}\hat{\Pi}_{z\sigma}G_{n\sigma}^{(0)}(q), \tag{51a}$$

$$\hat{F}_n^{\dagger(0)}(q) = -(i\hat{\sigma}_y)\sum_{\sigma=\uparrow,\downarrow}\hat{\Pi}_{z\sigma}F_{n\sigma}^{\dagger(0)}(q), \tag{51b}$$

where $\hat{\Pi}_{z\uparrow,\downarrow} = (1 \pm \hat{\sigma}_z)/2$ are the projection operators, and the expressions for the components read as

$$G_{n\sigma}^{(0)}(q) = \frac{\gamma_\sigma(q)}{2}\left[\frac{i\tilde{\omega}_n + \sigma h}{\sqrt{f_\sigma^2 - (i\tilde{\omega}_n + \sigma h)^2}} + i\,\mathrm{sgn}(q)\right], \tag{52a}$$

$$F_{n\sigma}^{\dagger(0)}(q) = \frac{\gamma_\sigma(q)}{2}\frac{f_\sigma}{\sqrt{f_\sigma^2 - (i\tilde{\omega}_n + \sigma h)^2}}, \tag{52b}$$

with $\gamma_\sigma(q) = \exp[-\sqrt{f_\sigma^2 - (i\tilde{\omega}_n + \sigma h)^2}|q|]$. The other Green's functions $\hat{\bar{G}}_n^{(0)}$ and $\hat{F}_n^{(0)}$ can be obtained from Eqs. (51) by using the symmetry relations $\hat{\bar{G}}_n^{(0)}(\omega_n) = -\hat{G}_n^{(0)}(-\omega_n)$ and $\hat{F}_n^{(0)}(\omega_n) = [\hat{F}_n^{\dagger(0)}(\omega_n)]^{\mathrm{T}}$.

The first-order correction for the Green's function at $q = 0$ is determined from the expression

$$\check{G}_n^{(1)}(q=0) = \int dq'\check{G}_n^{(0)}(-q')e\mathbf{v}_{Fn}\mathbf{A}(\mathbf{R} + q'\mathbf{v}_{Fn})\check{G}_n^{(0)}(q'). \tag{53}$$

We put

$$\mathbf{A}(\mathbf{R}) = \int\frac{d^2\mathbf{p}}{(2\pi)^2}\,\mathbf{A}(\mathbf{p})e^{i\mathbf{p}\mathbf{R}}, \tag{54a}$$

$$\mathbf{j}(\mathbf{R}) = \int\frac{d^2\mathbf{p}}{(2\pi)^2}\,\mathbf{j}(\mathbf{p})e^{i\mathbf{p}\mathbf{R}}, \tag{54b}$$

and then substitute Eqs. (51) and (52) into Eq. (53). Performing the integration, we derive a linear relation between the supercurrent and vector potential in the clean limit

$$\mathbf{j}(\mathbf{p}) = -e^2p_{Fn}v_{Fn}T\sum_{\omega_n}\sum_{\sigma=\uparrow,\downarrow}\frac{1}{2}\frac{f_\sigma^2}{\sqrt{f_\sigma^2 - (i\tilde{\omega}_n + \sigma h)^2}} \times\int\frac{d\mathbf{n}}{(2\pi)}\frac{\mathbf{n}(\mathbf{n}\mathbf{A}(\mathbf{p}))}{\left[f_\sigma^2 - (i\tilde{\omega}_n + \sigma h)^2 + v_{Fn}^2(\mathbf{n}\mathbf{p})^2/4\right]}. \tag{55}$$

Under the assumption of a local response, the above equation transforms as follows:

$$\mathbf{j}(\mathbf{R}) = -Q\mathbf{A}(\mathbf{R}), \tag{56a}$$

$$Q = e^2\frac{p_{Fn}v_{Fn}}{4}T\sum_{\omega_n,\sigma}\frac{f_\sigma^2}{\left[f_\sigma^2 - (i\tilde{\omega}_n + \sigma h)^2\right]^{3/2}}. \tag{56b}$$

Typical temperature dependencies of the coefficient Q in the linear relation (56) are shown in Fig. 4. For the sake of simplicity, we choose the interlayer gap function d_t to be constant within the considered temperature range. To take into account the temperature dependence of the gap function in the SC layer, we use the standard interpolation formula [56]

$$\Delta_s(T) = \Delta_0\tanh\left[1.74\sqrt{\frac{T_c}{T} - 1}\right], \tag{57}$$

where $\Delta_0 = \Delta_s(T=0)$ and T_c denotes the superconducting critical temperature. Figures 4(a)–4(c) show several $Q(T)$ plots for a fixed interlayer gap function and several tunneling rates $t^2/\Delta_0 = 0.1$, 0.2, 0.3, 0.4, and 0.5. The results in Fig. 4(a) for $d_t = 0$ indicate that in the absence of the

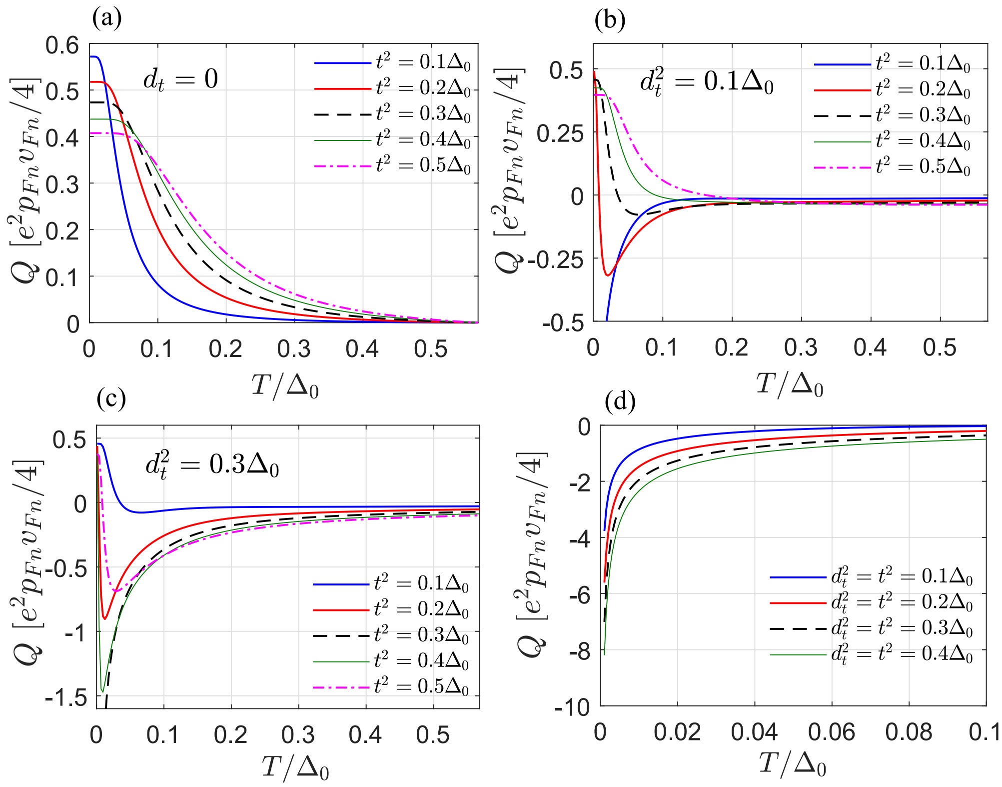

FIG. 4. Typical temperature dependencies of the coefficient Q in the linear relation between the supercurrent and the vector potential (56a). The plots represent the results of Eq. (56b), which is valid in the clean limit and under the assumption of a local response. (a), (b), and (c) correspond to $d_t^2 = 0, 0.1\Delta_0$, and $0.3\Delta_0$, respectively. (d) Several $Q(T)$ plots for $t^2 = d_t^2 = 0.1\Delta_0, 0.2\Delta_0, 0.3\Delta_0$, and $0.4\Delta_0$. Eq. (57) has been used to interpolate $\Delta_s(T)$ dependence whereas we choose the interlayer pairing amplitude d_t to be constant throughout the considered temperature range. Here $\Delta_0 = \Delta_s(T = 0)$.

interlayer spin-triplet pairing the induced superconducting correlations in 2DEG only exhibit the Meissner response ($Q > 0$). Diamagnetic response of the induced Cooper pairs becomes more pronounced at lower temperatures with decreasing t^2. This behavior is consistent with the fact that the induced gap in the quasiparticle energy spectrum of the two-dimensional layer decreases upon the decrease in the tunneling rate. $Q(T)$ plots in Figs. 4(b) and 4(c) reveal several qualitatively different types of the linear response within different temperature ranges. For $d_t^2 = t^2 = 0.1\Delta_0$ and $0.3\Delta_0$ [see a blue solid line in Fig. 4(b) and a black dashed line in Fig. 4(c)], the superconducting correlations in 2DEG exhibit the paramagnetic response ($Q < 0$) within the considered temperature range, and $|Q|$ grows with decreasing temperature. We note that this behavior is in qualitative agreement with our calculations of the density of states in the previous section, which yield a zero-bias anomaly at $t^2 \approx d_t^2$. The parameter range $t^2 > d_t^2$ ($t^2 < d_t^2$) is characterized by the presence of the minimum on a $Q(T)$ curve and a diamagnetic response at low temperatures. For clarity, we also reveal the low-temperature behavior of Q for $d_t^2 = t^2 = 0.1\Delta_0$, $0.2\Delta_0$, $0.3\Delta_0$, and $0.4\Delta_0$ in Fig. 4(d). Note that the presence of the paramagnetic response of 2DEG at high temperatures in Figs. 4(b) and 4(c) is related to the presence of the spin-triplet superconducting correlations in 2DEG, which actually survive in the limit $\Delta_s \to 0$.

2. Dirty limit

We proceed with investigating the linear response of the induced superconducting correlations in 2DEG with randomly distributed nonmagnetic point impurities. The effects of an elastic scattering are described by the impurity self-energy

$$\check{\Sigma}_{\rm imp}(\mathbf{R}) = \frac{1}{\tau}\int \frac{d\xi_n}{2\pi}\frac{d\mathbf{n}}{2\pi}\check{\tau}_z \check{G}_n(\mathbf{R}, \mathbf{n}, \xi_n)\check{\tau}_z, \tag{58}$$

included into Eq. (46). Here τ is the average time between collisions.

As a first step, we derive the Eilenberger equations for ξ_n-integrated Green's functions. For this purpose, we subtract Eq. (46) and its transpose. As a result, we get

$$-i\mathbf{v}_{Fn}\nabla_{\mathbf{R}}\check{g}_n(\mathbf{R}, \mathbf{n}) - [\check{w}(\mathbf{R}), \check{g}_n(\mathbf{R}, \mathbf{n})] = 0, \tag{59}$$

where

$$\check{w} = \check{\tau}_z[i\omega_n + \check{\Sigma}(\mathbf{R}) + \check{\Sigma}_{\rm imp}(\mathbf{R}) + e\mathbf{v}_{Fs}\mathbf{A}(\mathbf{R})], \tag{60}$$

and the quasiclassical Green's function is defined as follows:

$$\check{g}_n(\mathbf{R}, \mathbf{n}) = \int \frac{d\xi_n}{2\pi}\check{G}_n(\mathbf{R}, \mathbf{n}, \xi_n)\check{\tau}_z. \tag{61}$$

Using Eqs. (48), (51), and (52) evaluated at $q = 0$, it is straightforward to show that the introduced quasiclassical Green's function (61) obeys the normalization condition $\check{g}_n^2 = -1/4$. In this subsection we consider the case when the mean

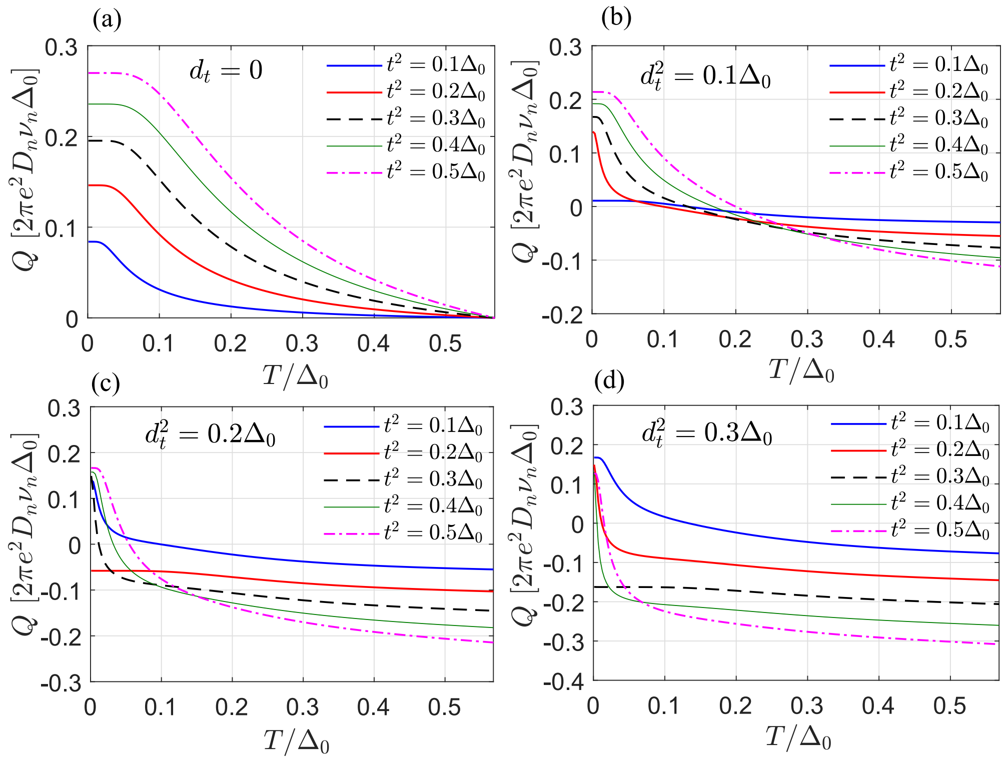

FIG. 5. Typical temperature dependencies of the coefficient Q in the linear relation (66a). The plots are the results of Eq. (66b), which is valid in the dirty limit. (a), (b), (c), and (d) correspond to $d_t^2 = 0$, $0.1\Delta_0$, $0.2\Delta_0$ and $0.3\Delta_0$, respectively. Eq. (57) has been used to interpolate $\Delta_s(T)$ dependence whereas we choose the interlayer pairing amplitude d_t to be constant throughout the considered temperature range.

free path for elastic scattering ℓ is much less than the spatial scale of the superconducting correlations in 2DEG. In this case one can seek the solution of Eq. (59) in the form

$$\check{g}_n(\mathbf{R}, \mathbf{n}) = \check{g}_n^{(0)}(\mathbf{R}) + \mathbf{n}\check{\mathbf{\Gamma}}_n(\mathbf{R}). \tag{62}$$

Isotropic part of the Green function $\check{g}_n^{(0)}$ satisfies the Usadel equation

$$D_n \check{\boldsymbol{\nabla}}_{\mathbf{R}}\big[\check{g}_s^{(0)}\check{\boldsymbol{\nabla}}_{\mathbf{R}}\check{g}_s^{(0)}\big] - \tfrac{1}{2}\big[\check{\tau}_z(i\omega_n + \check{\Sigma}), \check{g}_s^{(0)}\big] = 0, \tag{63}$$

whereas a small correction $\check{\mathbf{\Gamma}}_n$ is determined from the expression

$$\check{\mathbf{\Gamma}}_n(\mathbf{R}) = 2i\ell\check{g}_n^{(0)}(\mathbf{R})\check{\boldsymbol{\nabla}}_{\mathbf{R}}\check{g}_n^{(0)}(\mathbf{R}). \tag{64}$$

In the above equations $\check{\boldsymbol{\nabla}}_{\mathbf{R}}\check{a} = \boldsymbol{\nabla}_{\mathbf{R}}\check{a} - ie\mathbf{A}[\check{\tau}_z, \check{a}]$ and $D_n = v_{Fn}\ell/2$ is the diffusion coefficient in 2DEG. Substituting Eqs. (62) and (64) into Eq. (47), we get the expression for the supercurrent

$$\begin{aligned}\mathbf{j}(\mathbf{R}) = &- 2ieD_n\nu_n T\sum_{\omega_n}\mathrm{Tr}\big[\hat{g}_n^{(0)}(\mathbf{R})\boldsymbol{\nabla}_{\mathbf{R}}\hat{g}_n^{(0)}(\mathbf{R}) \\ &+ \hat{f}_n^{(0)}(\mathbf{R})(\boldsymbol{\nabla}_{\mathbf{R}} + 2ie\mathbf{A}(\mathbf{R}))\hat{f}_n^{\dagger(0)}(\mathbf{R})\big].\end{aligned} \tag{65}$$

Note that for the chosen gauge of the vector potential div$\mathbf{A} = 0$, the Usadel equation (63) doesn't contain linear terms in $\mathbf{A}$. Correspondingly, the linear relation between the supercurrent and the vector potential can be obtained by substituting the zero-order spatially homogeneous Green's functions defined by Eqs. (51) and (52) into Eq. (65). As a result, we obtain the local relation

$$\mathbf{j}(\mathbf{R}) = -Q\mathbf{A}(\mathbf{R}), \tag{66a}$$

$$Q = 2\pi e^2 D_n\nu_n T\sum_{\omega_n}\sum_{\sigma=\uparrow,\downarrow}\frac{f_\sigma^2}{\big[f_\sigma^2 - (i\tilde{\omega}_n + \sigma h)^2\big]}. \tag{66b}$$

Typical temperature dependencies of the coefficient Q in the linear relation (66a) are shown in Fig. 5. The plots are the results of Eq. (66b). Panels (a), (b), (c), and (d) correspond to $d_t^2/\Delta_0 = 0$, 0.1, 0.2, and 0.3, respectively. Figure 5(a) shows that in the absence of the spin-triplet interlayer pairing the induced superconducting correlations in 2DEG only exhibit the diamagnetic response. In contrast with the corresponding results for the clean limit [see Fig. 4(a)], the plots in Fig. 5(a) demonstrate that the magnitude of the response $|Q|$ at low temperatures grows with increasing tunneling rate. Similarly to the previously considered case, we find that in the case of a finite interlayer gap function the type of the linear response can vary with temperature. In particular, the results for $d_t^2 = t^2 = 0.1\Delta_0$ [shown by a blue solid line in Fig. 5(b)] reveal rather small diamagnetic response at low temperatures, which switches into the paramagnetic one upon the increase in T. The increase in the tunneling rate t^2 results in the enhancement of both the diamagnetic and paramagnetic response. The temperature range corresponding to the diamagnetic response increases for larger tunneling rates. Panels (c) and (d) show typical $Q(T)$ plots within both parameter regions $t^2 < d_t^2$ and $t^2 > d_t^2$. Considering, for instance, Fig. 5(d), we see that for $t^2 = 0.1\Delta_0$ the two-dimensional layer features the diamagnetic (paramagnetic) response at low (high) temperatures. The temperature range, within which the Meissner response is established shrinks upon the increase in t^2. At $t^2 = d_t^2 = 0.3\Delta_0$ [see a black dashed line in Fig. 5(d)] 2DEG exhibits the paramagnetic response within the considered temperature range. Further increase in the tunneling rate $t^2 > d_t^2$ restores the low-temperature diamagnetic response and also leads to the enhancement of the paramagnetic response at high temperatures.

IV. CONCLUDING REMARKS

Finally, let us comment on the relation between the direct and inverse proximity effect in superconductor-normal metal structures. In a standard situation rather high transparency of the barrier between the subsystems implies a strong inverse proximity effect. Our results point out that in the presence of the interlayer pairing this relation can break down, namely the inverse proximity effect can be small whereas experimentally measurable effects of the induced superconducting correlations can be noticeable. Note that some indications of such phenomena have been recently observed in [57].

To sum up, we have studied the manifestations of the interlayer pairing in proximitized heterostructures. Depending on the geometry and dimensionality of the system, we have shown that the interlayer pairing can lead to the appearance of the odd-frequency superconducting correlations, FFLO instability, the paramagnetic contribution to the Meissner response, and the multi-peak structure of the density of states. We believe that the obtained results can be useful both for the analysis of experimental data on proximitized heterostructures and for engineering new types of superconducting states in systems with induced superconductivity. Since the considered mechanism can play a role of the Zeeman field, it can be possible that the related effects can be useful for development of new platforms for topologically protected qubits based on Majorana modes [9,10].

ACKNOWLEDGMENTS

This work was supported by the Russian Science Foundation (Grant No. 20-12-00053) in part related to the analysis of the spin-triplet interlayer pairing in the two-dimensional electron gas coupled to a massive superconductor, the Foundation for the Advancement of Theoretical Physics and Mathematics BASIS (Grant No. 23-1-2-32) in part related to the analysis of the spin-singlet interlayer superconductivity in the two-layer model, and the Center of Excellence "Center of Photonics" funded by the Ministry of Science and Higher Education of the Russian Federation (Contract No. 075-15-2022-316) in part related to the analysis of the screening properties of the two-layer system).

APPENDIX: DERIVATION OF EQS. (28) IN THE MAIN TEXT

Throughout the second part of our work we use the following Green's functions:

$$\check{G}_s(\mathbf{X}_1, \mathbf{X}_2) = \langle T_\tau \check{\psi}_s(\mathbf{X}_1)\check{\psi}_s^\dagger(\mathbf{X}_2)\rangle, \tag{A1a}$$

$$\check{G}_n(\mathbf{x}_1, \mathbf{x}_2) = \langle T_\tau \check{\psi}_n(\mathbf{x}_1)\check{\psi}_n^\dagger(\mathbf{x}_2)\rangle, \tag{A1b}$$

$$\check{G}_t(\mathbf{X}_1, \mathbf{x}_2) = \langle T_\tau \check{\psi}_s(\mathbf{X}_1)\check{\psi}_n^\dagger(\mathbf{x}_2)\rangle, \tag{A1c}$$

$$\check{\mathcal{G}}_t(\mathbf{x}_1, \mathbf{X}_2) = \langle T_\tau \check{\psi}_n(\mathbf{x}_1)\check{\psi}_s^\dagger(\mathbf{X}_2)\rangle. \tag{A1d}$$

Here $\mathbf{x} = (\mathbf{r}, \tau)$ and $\mathbf{X} = (\mathbf{R}, \tau)$, τ is the imaginary time variable in the Matsubara technique, T_τ is the time-ordering operator. We define the Nambu spinors $\check{\psi}_s(\mathbf{X})$ and $\check{\psi}_n(\mathbf{x})$ as

$$\check{\psi}_s(\mathbf{X}) = [\psi_{s\uparrow}(\mathbf{X}), \psi_{s\downarrow}(\mathbf{X}), \psi_{s\uparrow}^\dagger(\mathbf{X}), \psi_{s\downarrow}^\dagger(\mathbf{X})]^{\mathrm{T}}, \tag{A2a}$$

$$\check{\psi}_n(\mathbf{x}) = [\psi_{n\uparrow}(\mathbf{x}), \psi_{n\downarrow}(\mathbf{x}), \psi_{n\uparrow}^\dagger(\mathbf{x}), \psi_{n\downarrow}^\dagger(\mathbf{x})]^{\mathrm{T}}. \tag{A2b}$$

Below we present the equations of motion for the field operators and the derivation of the Gor'kov equations in the absence of the external magnetic field. Note that in this section we don't restrict ourselves with a spatially homogeneous hopping parameter and superconducting order parameters. For the considered model (23), fermionic operators in the SC layer satisfy the equations of motion

$$\begin{aligned}\frac{\partial}{\partial\tau}\check{\psi}_s(\mathbf{X}) = &-[\check{\tau}_z\xi_s(\mathbf{R}) + \check{\Delta}_s(\mathbf{R})]\check{\psi}_s(\mathbf{X}) - d\delta(Z)t(\mathbf{r})\check{\tau}_z\check{\psi}_n(\mathbf{x})\\ &-\frac{U_0}{2}d\delta(Z)\check{\tau}_z[\psi_{n\sigma}^\dagger(\mathbf{x})\psi_{n\sigma}(\mathbf{x})]\check{\psi}_s(\mathbf{X}),\end{aligned} \tag{A3}$$

where $\check{\tau}_i$ $(i = x, y, z)$ are the Pauli matrices acting in the particle-hole space and the superconducting gap matrix has the form

$$\check{\Delta}_s(\mathbf{R}) = \begin{bmatrix} 0 & \hat{\Delta}_s(\mathbf{R}) \\ \hat{\Delta}_s^\dagger(\mathbf{R}) & 0 \end{bmatrix}, \tag{A4}$$

Here $\hat{\Delta}_s(\mathbf{R}) = (i\hat{\sigma}_y)\Delta_s(\mathbf{R})$, $\hat{\sigma}_i$ $(i = x, y, z,)$ are the Pauli matrices acting in the spin space. Equations of motion for the field operators in 2DEG are as follows:

$$\begin{aligned}\frac{\partial}{\partial\tau}\check{\psi}_n(\mathbf{x}) = &-\check{\tau}_z\xi_n(\mathbf{r})\check{\psi}_n(\mathbf{x}) - t(\mathbf{r})\check{\tau}_z\check{\psi}_s(\mathbf{x})\\ &-\frac{U_0}{2}\check{\tau}_z[\psi_{s\sigma}^\dagger(\mathbf{x})\psi_{s\sigma}(\mathbf{x})]\check{\psi}_n(\mathbf{x}).\end{aligned} \tag{A5}$$

For the derivation of the Gor'kov equations for the Green's functions (A1), one should decouple thermodynamic averages of four fermionic operators [52]. For instance, considering the equation for the normal correlation function in 2DEG $[\hat{G}_n]_{\alpha\beta}$, we have the combinations

$$\begin{aligned}&\langle T_\tau\psi_{s\sigma}^\dagger(\mathbf{x}_1)\psi_{s\sigma}(\mathbf{x}_1)\psi_{n\alpha}(\mathbf{x}_1)\psi_{n\beta}^\dagger(\mathbf{x}_2)\rangle\\ &= \langle T_\tau\psi_{s\sigma}^\dagger(\mathbf{x}_1)\psi_{s\sigma}(\mathbf{x}_1)\rangle\langle T_\tau\psi_{n\alpha}(\mathbf{x}_1)\psi_{n\beta}^\dagger(\mathbf{x}_2)\rangle\\ &\quad - \langle T_\tau\psi_{s\sigma}^\dagger(\mathbf{x}_1)\psi_{n\alpha}(\mathbf{x}_1)\rangle\langle T_\tau\psi_{s\sigma}(\mathbf{x}_1)\psi_{n\beta}^\dagger(\mathbf{x}_2)\rangle\\ &\quad + \langle T_\tau\psi_{s\sigma}^\dagger(\mathbf{x}_1)\psi_{n\beta}^\dagger(\mathbf{x}_2)\rangle\langle T_\tau\psi_{s\sigma}(\mathbf{x}_1)\psi_{n\alpha}(\mathbf{x}_1)\rangle.\end{aligned} \tag{A6}$$

In the present work, we focus on the effects of the interlayer anomalous averages represented, for instance, by the last term in the right-hand side of Eq. (A6) and neglect the other contributions. Using Eqs. (A1) and (A5), we derive the equations for the Matsubara Green's functions in 2DEG

$$\begin{aligned}&\left[\frac{\partial}{\partial\tau_1} + \check{\tau}_z\xi_n(\mathbf{r}_1)\right]\check{G}_n(\mathbf{x}_1, \mathbf{x}_2) + \check{t}(\mathbf{r}_1)\check{G}_t(\mathbf{x}_1, \mathbf{x}_2)\\ &= d^{-1}\delta(\mathbf{x}_1 - \mathbf{x}_2),\end{aligned} \tag{A7}$$

where the coupling matrix

$$\check{t}(\mathbf{r}) = \begin{pmatrix} t(\mathbf{r}) & \hat{\Delta}_{\mathrm{int}}(\mathbf{r}) \\ -\hat{\Delta}_{\mathrm{int}}^*(\mathbf{r}) & -t(\mathbf{r}) \end{pmatrix}, \tag{A8}$$

acquires a nontrivial structure in the particle-hole space due to the presence of the interlayer gap function

$$[\hat{\Delta}_{\rm int}(\mathbf{r})]_{\alpha\beta} = -\frac{U_0}{2}\langle\psi_{n\alpha}(\mathbf{x})\psi_{s\beta}(\mathbf{x})\rangle. \tag{A9}$$

Equations for the Green's functions can be more conveniently in the Matsubara frequency representation $\omega_n = 2\pi T(n + 1/2)$. We set $\tau = \tau_1 - \tau_2$ and write

$$\check{G}(\mathbf{r}_1, \mathbf{r}_2) = \int_0^{1/T} d\tau\ \check{G}(\mathbf{x}_1, \mathbf{x}_2)e^{i\omega_n\tau}, \tag{A10}$$

omitting the frequency argument for brevity. Equations for the Green's functions in 2DEG written in the Matsubara frequency-coordinate representation have the form

$$\begin{aligned}[-i\omega_n + \check{\tau}_z\xi_n(\mathbf{r}_1)]\check{G}_n(\mathbf{r}_1, \mathbf{r}_2) + \check{t}(\mathbf{r}_1)\check{G}_t(\mathbf{r}_1, \mathbf{r}_2)\\ = d^{-1}\delta(\mathbf{r}_1 - \mathbf{r}_2).\end{aligned} \tag{A11}$$

We derive the equation for the tunneling Green function in a similar fashion

$$\begin{aligned}[-i\omega_n + \check{\tau}_z\xi_s(\mathbf{R}_1) + \check{\Delta}_s(\mathbf{R}_1)]\check{G}_t(\mathbf{R}_1, \mathbf{r}_2)\\ + d\delta(Z_1)\check{t}^\dagger(\mathbf{r}_1)\check{G}_n(\mathbf{r}_1, \mathbf{r}_2) = 0.\end{aligned} \tag{A12}$$

Neglecting the back action of 2DEG on the superconductor and the effects of the interlayer interaction in the SC layer, the Gor'kov equations in the SC layer read

$$[-i\omega_n + \check{\tau}_z\xi_s(\mathbf{R}_1) + \check{\Delta}_s(\mathbf{R}_1)]\check{G}_s(\mathbf{R}_1, \mathbf{R}_2) = \delta(\mathbf{R}_1 - \mathbf{R}_2). \tag{A13}$$

To obtain a closed system of equations for the Green's functions in 2DEG we follow Ref. [54] and write the solution of Eq. (A12)

$$\check{G}_t(\mathbf{R}_1, \mathbf{r}_2) = -d\int d^2\mathbf{r}'\check{G}_s(\mathbf{R}_1, \mathbf{r}')\check{t}^\dagger(\mathbf{r}')\check{G}_n(\mathbf{r}', \mathbf{r}_2). \tag{A14}$$

Substituting Eq. (A14) into Eq. (A11), we derive Eqs. (28) in the main text.

[1] W. L. McMillan, Tunneling model of the superconducting proximity effect, Phys. Rev. **175**, 537 (1968).
[2] A. I. Buzdin, Proximity effects in superconductor-ferromagnet heterostructures, Rev. Mod. Phys. **77**, 935 (2005).
[3] F. S. Bergeret, A. F. Volkov, and K. B. Efetov, Odd triplet superconductivity and related phenomena in superconductor-ferromagnet structures, Rev. Mod. Phys. **77**, 1321 (2005).
[4] V. M. Edelstein, Triplet superconductivity and magnetoelectric effect near the s-wave-superconductor–normal-metal interface caused by local breaking of mirror symmetry, Phys. Rev. B **67**, 020505(R) (2003).
[5] M. Eschrig, Spin-polarized supercurrents for spintronics: A review of current progress, Rep. Prog. Phys. **78**, 104501 (2015).
[6] J. Linder and J. W. A. Robinson, Superconducting spintronics, Nat. Phys. **11**, 307 (2015).
[7] I. V. Bobkova, A. M. Bobkov, and M. A. Silaev, Magnetoelectric effects in Josephson junctions, J. Phys.: Condens. Matter **34**, 353001 (2022).
[8] A. S. Mel'nikov, S. V. Mironov, A. V. Samokhvalov, and A. I. Buzdin, Superconducting spintronics: State of the art and prospects, Phys. Usp. **65**, 1248 (2022).
[9] C. Nayak, S. H. Simon, A. Stern, M. Freedman, and S. Das Sarma, Non-Abelian anyons and topological quantum computation, Rev. Mod. Phys. **80**, 1083 (2008).
[10] S. Das Sarma, M. Freedman, and C. Nayak, Majorana zero modes and topological quantum computation, npj Quantum Inf. **1**, 15001 (2015).
[11] K. B. Efetov and A. I. Larkin, Pairing with nonzero spin in layered and in quasi-one-dimensional superconductors, Zh. Eksp. Teor. Fiz. **68**, 155 (1975) [Sov. Phys. JETP **41**, 76 (1975)].
[12] Z. Tešanović, Role of interlayer coupling in oxide superconductors, Phys. Rev. B **36**, 2364(R) (1987).
[13] L. N. Bulaevskii and M. V. Zyskin, Energy gap in layered superconductors, Phys. Rev. B **42**, 10230 (1990).
[14] R. A. Klemm and S. H. Liu, Intralayer-versus-interlayer pairing in the copper oxide superconductors, Phys. Rev. B **44**, 7526 (1991).
[15] S. H. Liu and R. A. Klemm, Intralayer versus interlayer pairing in the copper oxide superconductors: The three- and four-layer problems, Phys. Rev. B **45**, 415 (1992).
[16] S. Kettemann and K. B. Efetov, Interlayer pairing in layered superconductors, Phys. Rev. B **46**, 8515 (1992).
[17] J. Bardeen, L. N. Cooper, and J. R. Schrieffer, Theory of Superconductivity, Phys. Rev. **108**, 1175 (1957).
[18] R. C. Morris and R. V. Coleman, Anisotropic Superconductivity in Layer Compounds, Phys. Rev. B **7**, 991 (1973).
[19] K. Deguchi, Y. Takano, and Y. Mizuguchi, Physics and chemistry of layered chalcogenide superconductors, Sci. Technol. Adv. Mater. **13**, 054303 (2012).
[20] D. L. Duong, S. J. Yun, and Y. H. Lee, Van der Waals Layered materials: opportunities and challenges, ACS Nano **11**, 11803 (2017).
[21] A. Jindal, A. Saha, Z. Li, T. Taniguchi, K. Watanabe, J. C. Hone, T. Birol, R. M. Fernandes, C. R. Dean, A. N. Pasupathy, and D. A. Rhodes, Coupled ferroelectricity and superconductivity in bilayer T_d-$MoTe_2$, Nature (London) **613**, 48 (2023).
[22] M. V. Hosseini and M. Zareyan, Model of an exotic chiral superconducting phase in a graphene bilayer, Phys. Rev. Lett. **108**, 147001 (2012).
[23] M. V. Hosseini and M. Zareyan, Unconventional superconducting states of interlayer pairing in bilayer and trilayer graphene, Phys. Rev. B **86**, 214503 (2012).
[24] C.-X. Liu, Unconventional superconductivity in bilayer transition metal dichalcogenides, Phys. Rev. Lett. **118**, 087001 (2017).
[25] M. Alidoust, M. Willatzen, and A.-P. Jauho, Symmetry of superconducting correlations in displaced bilayers of graphene, Phys. Rev. B **99**, 155413 (2019).
[26] A. O. Sboychakov, A. L. Rakhmanov, A. V. Rozhkov, Superconductivity and spin density wave in AA stacked bilayer graphene, arXiv:2311.07405.
[27] E. Thingstad, J. Hutchinson, Daniel Loss, and J. Klinovaja, Topological interlayer superconductivity in a van der Waals heterostructure, arXiv:2405.07927.

[28] B. S. Chandrasekhar, A note on the maximum critical field of high-field superconductors, Appl. Phys. Lett. **1**, 7 (1962).

[29] A. M. Clogston, Upper limit for the critical field in hard superconductors, Phys. Rev. Lett. **9**, 266 (1962).

[30] D. Saint-James, G. Sarma, and E. J. Thomas, *Type II Superconductivity, Commonwealth and International Library. Liberal Studies Divi* (Elsevier, Science & Technology, New York, 1969).

[31] P. Fulde and R. A. Ferrel, Superconductivity in a strong spin-exchange field, Phys. Rev. **135**, A550 (1964).

[32] A. I. Larkin and Y. N. Ocvhinnikov, Nonuniform state of superconductors, Zh. Eksp. Teor. Fiz. **47**, 1136 (1964) [Sov. Phys. JETP **20**, 762 (1965)].

[33] J. Linder and A. V. Balatsky, Odd-frequency superconductivity, Rev. Mod. Phys. **91**, 045005 (2019).

[34] P. Visani, A. C. Mota, and A. Pollini, Novel reentrant effect in the proximity-induced superconducting behavior of silver, Phys. Rev. Lett. **65**, 1514 (1990).

[35] F. B. Müller-Allinger and A. C. Mota, Paramagnetic reentrant effect in high purity mesoscopic AgNb proximity structures, Phys. Rev. Lett. **84**, 3161 (2000).

[36] C. Bruder and Y. Imry, Orbital paramagnetism of electrons in proximity to a superconductor, Phys. Rev. Lett. **80**, 5782 (1998).

[37] A. L. Fauchère, W. Belzig, andd G. Blatter, Paramagnetic instability at normal-metal–superconductor interfaces, Phys. Rev. Lett. **82**, 3336 (1999).

[38] K. Maki and S. Haas, Paramagnetic reentrance effect in NS proximity cylinders, Phys. Lett. A **272**, 271 (2000).

[39] C. Espedal, T. Yokoyama, and J. Linder, Anisotropic paramagnetic meissner effect by spin-orbit coupling, Phys. Rev. Lett. **116**, 127002 (2016).

[40] S. M. Albrecht, A. P. Higginbotham, M. Madsen, F. Kuemmeth, T. S. Jespersen, J. Nygård, P. Krogstrup, and C. M. Marcus, Exponential protection of zero modes in Majorana islands, Nature (London) **531**, 206 (2016).

[41] J. D. S. Bommer, H. Zhang, Ö. Gül, B. Nijholt, M. Wimmer, F. N. Rybakov, J. Garaud, D. Rodic, E. Babaev, M. Troyer, D. Car, S. R. Plissard, E. P. A. M. Bakkers, K. Watanabe, T. Taniguchi, and L. P. Kouwenhoven, Spin-orbit protection of induced superconductivity in majorana nanowires, Phys. Rev. Lett. **122**, 187702 (2019).

[42] A. A. Vargas-Paredes, A. A. Shanenko, A. Vagov, M. V. Milošević, and A. Perali, Crossband versus intraband pairing in superconductors: Signatures and consequences of the interplay, Phys. Rev. B **101**, 094516 (2020).

[43] G. Midei and A. Perali, Sweeping across the BCS-BEC crossover, reentrant, and hidden quantum phase transitions in two-band superconductors by tuning the valence and conduction bands, Phys. Rev. B **107**, 184501 (2023).

[44] I. V. Blinov and A. H. MacDonald, Interlayer coherence in superconductor bilayers, Phys. Rev. B **106**, 224504 (2022).

[45] S. Tewari, T. D. Stanescu, J. D. Sau, and S. Das Sarma, Topologically non-trivial superconductivity in spin–orbit-coupled systems: Bulk phases and quantum phase transitions, New J. Phys. **13**, 065004 (2011).

[46] N. Kopnin, *Theory of Nonequilibrium Superconductivity* (Oxford University Press, Oxford, 2001).

[47] A. Buzdin, S. Tollis, and J. Cayssol, Field-induced superconductivity with an enhanced and tunable paramagnetic limit, Phys. Rev. Lett. **95**, 167003 (2005).

[48] A. A. Abrikosov, *Fundamentals of the Theory of Metals*, (Courier Dover Publications, Mineola, New York, 2017).

[49] R. Heid, On the thermodynamic stability of odd-frequency superconductors, Z. Phys. B **99**, 15 (1995).

[50] D. Solenov, I. Martin, and D. Mozyrsky, Thermodynamical stability of odd-frequency superconducting state, Phys. Rev. B **79**, 132502 (2009).

[51] Ya. V. Fominov, Y. Tanaka, Y. Asano, and M. Eschrig, Odd-frequency superconducting states with different types of Meissner response: Problem of coexistence, Phys. Rev. B **91**, 144514 (2015).

[52] A. A. Abrikosov, L. P. Gorkov, and I. E. Dzyaloshinski, *Methods of Quantum Field Theory in Statistical Physics* (Prentice Hall, Englewood Cliffs, New Jersey, 1963).

[53] F. Parhizgar and A. M. Black-Schaffer, Diamagnetic and paramagnetic Meissner effect from odd-frequency pairing in multiorbital superconductors, Phys. Rev. B **104**, 054507 (2021).

[54] N. B. Kopnin and A. S. Melnikov, Proximity-induced superconductivity in two-dimensional electronic systems, Phys. Rev. B **84**, 064524 (2011).

[55] A. V. Svidzinski, *Space-Inhomogeneous Problems in the Theory of Superconductivity* (Nauka, Moscow, 1982).

[56] F. Gross, B. S. Chandrasekhar, D. Einzel, K. Andreas, P. J. Hirschfeld, H. R. Ott, J. Beuers, Z. Fisk, and J. L. Smith, Anomalous temperature dependence of the magnetic field penetration depth in superconducting UBe_{13}, Z. Phys. B **64**, 175 (1986).

[57] E. E. Pestov, Yu. N. Nozdrin, V. V. Rogov, I. Yu. Pashen'kin, and D. Yu. Vodolazov, Peculiarities of the nonlinear response of a superconductor–normal metal structure with a large ratio of resistivities, Phys. Solid State **61**, 1539 (2019).